Hindawi
Complexity
Volume 2021, Article ID 6635571, 16 pages
https://doi.org/10.1155/2021/6635571

Research Article

Simple Adaptive Control-Based Reconfiguration Design of Cabin Pressure Control System

Zhao Zhang,[1] **Zhong Yang**,[1] **Si Xiong**,[1,2] **Shuang Chen**,[3] **Shuchang Liu**,[1] **and Xiaokai Zhang**[3]

[1] *College of Automation Engineering, Nanjing University of Aeronautics and Astronautics, Nanjing 211106, China*
[2] *COMAC Beijing Aircraft Technology Research Institute, Beijing 102211, China*
[3] *Electronic Engineering Department, Aviation Key Laboratory of Science and Technology on Aero Electromechanical System Integration, Nanjing 211106, China*

Correspondence should be addressed to Zhong Yang; yangzhong@nuaa.edu.cn

Received 18 December 2020; Revised 7 March 2021; Accepted 11 March 2021; Published 30 March 2021

Academic Editor: Danilo Comminiello

The Cabin Pressure Control System (CPCS) is an essential part of the aviation environmental control system that ensures aircraft structure and flight crew safety. However, the CPCS usually has potential faults of sensors and actuators. To this end, a Simple Adaptive Control- (SAC-) based reconfiguration method is proposed to compensate for the above adverse effects. Some good pressure control performance of CPCS can be achieved by the basic pressure controller when the system is in normal operation. A parallel feedforward compensator is designed to guarantee the closed-loop system's stability and the almost strictly positive realness of the augmented system. Thus, the simple adaptive controller can be utilized for the CPCS. In particular, the reconfiguration system can update the control law online when the fault occurs without the system identification process. The reference model is obtained by mathematical model linearization after considering the mechanical characteristics of the CPCS. Extensive simulations under various typical fault scenarios are carried out throughout the entire flight envelope of the aircraft from take-off to landing. Simulation results validate the robustness and reconfiguration control capability of the proposed method.

1. Introduction

The function of the Cabin Pressure Control System (CPCS) is to ensure that the cabin pressure and its change rate satisfy the specification requirement throughout the entire flight envelope [1]. However, in practical engineering, various components such as actuators, sensors, and processors of CPCS may confront failures during operation. The high-altitude low-pressure environment and the excessively high air pressure change rate will seriously endanger human health or even cause deaths [2]. A healthy CPCS is widely recognized to be the key to the safe completion of flight missions. To this end, some researches on the faulty CPCS have been carried out. In terms of practical engineering, Zhao et al. drew attention to some typical failures of aircraft environmental control systems and found that a small black impurity stuck the pressure regulating valve, which was the cause of the continuous decrease in cabin pressure and the pain of the pilot's eardrum [3]. DAI discussed the reasons for the abnormal phenomenon of cabin pressure and suggested some feasible recommendations after collecting the existing worldwide accident data [4]. To reduce the repetitive failures caused by the aging of CPCS components, some preventive maintenance measures were proposed by Jiang et al. [5]. In terms of numerical and theoretical analysis, Liu et al. provided a detailed analysis of the cabin pressure parameters in various conditions through simulating the normal and failure states of CPCS and thus concluded that the pilot must descend the aircraft to a safe altitude for avoiding the fatal accidents when CPCS failed [6]. It is easy to see that the demand for reliability, safety, and fault tolerance of the

CPCS is generally high. A faulty CPCS will seriously affect the completion of a flight mission.

To date, research on the CPCS controller has mostly focused on control method design, such as PID control [7], fuzzy control [8], fuzzy sliding mode variable structure control [9], and neural network adaptive control [10]. Although the pressure control effect has been improved, the approaches used have failed to provide a solution for the faults of CPCS. Previous studies also have failed to consider compensating the adverse effects caused by faulty CPCS from the perspective of controller design. Therefore, to improve the reliability and availability while providing the desired performance, it is necessary to design a control system that is capable of tolerating potential faults in the CPCS. This type of control system is often known as the fault-tolerant control system [11]. Thus, the research on fault-tolerant control of CPCS is an interesting and valuable topic according to the above analysis.

As a branch of fault-tolerant control, control reconfiguration is widely applied to some safety-critical systems at present, especially in the field of aerospace engineering [12]. The control reconfiguration technology for the control system in the presence of faults is a key way to realize the soft redundancy [13]. It can be divided into active reconfiguration and passive reconfiguration, based on Fault Detection and Identification (FDI) and FDI-free reconfiguration methods [14–16]. As one of the most popular control reconfiguration methods, the area of adaptive control is attracting increasing attention [17–19], and researchers have proposed many advanced methods combined with adaptive control [20–22]. In particular, a direct adaptive control method was proposed [23]. It has the advantages of both the active reconfiguration method and the FDI-free reconfiguration method [24–26], including no need to know the faulty situation in advance. The direct adaptive control method has been improved by researchers in a number of studies. Kim et al. improved the direct adaptive controller structure, thereby increasing the robustness of the controller [27]. Chai et al. proposed using the states of the reference model instead of its output as a part of the direct adaptive controller and avoided the missing information caused by multiplying the observation matrix [28]. However, the complexity of the aforementioned adaptive laws reduces the applicability of the proposed methods.

Simple Adaptive Control (SAC) developed by Sobel, Kaufman, and Mabius [29, 30] belongs to a model following-based direct adaptive control. SAC was successfully applied to control various plants [31, 32]. The main idea of SAC is to make the performance of the controlled system track the output of the predesigned reference model [33, 34]. Besides, the structure and parameters of the reference model need not be the same as the controlled system. Different from the previously proposed direct adaptive methods, the adaptive law of SAC only requires the reference model and tracking error information. SAC has been recognized as one of the most practical direct adaptive control methods due to its simple structure and few adjustable parameters [35]. In terms of fault-tolerant control, some outstanding reconfiguration researches based on SAC have been performed. Chen et al. proposed a reconfiguration control scheme based on SAC for a quadrotor helicopter with loss of control effectiveness and validated its robustness and reconfiguration control capability [36]. SAC method was extended by Belkharraz et al. and applied to reconfigure the F/A-18 aircraft model with a 50% loss of control effectiveness [37]. Results reported suggest that the proposed method exhibits improved model following. The aim of the study by Masanori Takahashi was to reduce the impact of sensor failures; a fault-tolerant SAC system is developed which could automatically replace the failed sensors with healthy backups to maintain its performance [38]. As can be seen from the above, SAC has satisfactory fault tolerance and is suitable for reconfiguration design.

Based on the existing researches, these key issues are proposed:

(i) The health condition of CPCS is generally regarded as the primary reason affecting flight safety. However, the previous researches on CPCS were limited to the control method design and actual system maintenance measures. The area of using fault-tolerant control methods to improve the reliability and safety of CPCS has not been explored in depth.

(ii) According to the previous reconfiguration researches, most of the reconfigured objects were flight control systems that generally belong to MIMO systems, while CPCS is SISO. Unfortunately, few studies have explored the reconfiguration of aviation electromechanical control systems (AECS) including CPCS.

(iii) All control systems may have potential faults of sensors, actuators, and so on. Nevertheless, the type of faults considered in most of the previous reconfiguration researches was mainly about loss of control effectiveness or rudder surface damage. In other words, it is too single and limited that the proposed methods do not have a strong universality.

Motivated by the above observations, a SAC-based reconfiguration method is proposed for CPCS subject to various potential faults. The reconfiguration control system contains a basic pressure controller and a simple adaptive controller for the faulty CPCS. Due to the widespread use in engineering, a PID controller is applied as the basic controller to ensure the good performance of CPCS. Before applying the SAC method, the condition of almost strictly positive realness of the closed-loop system must be satisfied when different faults occur in the CPCS. Thus, a parallel feedforward compensator is designed to guarantee the stability of the closed-loop system and the almost strictly positive realness of the augmented system. Different from the previously proposed reference model selection method, the linearized CPCS is directly adopted as the reference model in this paper so that the pressure tracking is more in line with the actual situation. And the reconfiguration performance can be better observed. In particular, the fault types considered in this paper are mainly sensor faults and actuator faults, which are the typical faults of CPCS.

Furthermore, some selecting principles of the control parameters which directly affect the reconfiguration performance are given after various simulation studies. From the potential application perspective, the proposed method has a strong universality. After considering the mechanical characteristics of many AECS, including cabin temperature control system [39], hydraulic control system [40], and landing gear steering control system [41], three common characteristics between them can be described as follows: (1) ensuring flight safety and quality; (2) SISO; (3) existing some potential faults. Therefore, the proposed method has the possibility to be applied to other AECS.

In summary, the contributions of this paper are highlighted as follows:

(i) A reconfiguration concept which belongs to fault-tolerant control is introduced to handle unknown faults.

(ii) A SAC-based reconfiguration method is proposed due to the characteristics of CPCS which include SISO and existing various potential faults.

(iii) A parallel feedforward compensator is designed to apply the SAC method when different faults occur in the CPCS.

(iv) A few selecting principles of the control parameters are given to improve the reconfiguration effect.

(v) The proposed method in this paper has a potential application in other AECS.

The paper structure is organized as follows: A mathematical model of CPCS is established, and a reference model is obtained through linearization. Secondly, SAC method is introduced to design the reconfiguration control system, and a parallel feedforward compensator is designed to guarantee the stability of the faulty CPCS, followed by its stability analysis. In the simulation, various typical faults are injected into CPCS for testing the proposed method. The simulation results reveal the robustness and excellent reconfiguration control capability of the proposed method.

2. Working Principle of CPCS

The CPCS is mainly composed of the signal comparator, cabin pressure controller, drive motor, exhaust valve, cabin pressure sensor, and aircraft cabin (as shown in Figure 1). The signal comparator receives the command pressure signal and the output signal of the cabin pressure sensor. Then, the error of the above two signals is sent to the cabin pressure controller. Ultimately, the actuator that consists of a drive motor and exhaust valve is controlled to change the exhaust valve's opening for adjusting exhaust volume, so that the cabin pressure can be controlled.

3. CPCS Modeling

3.1. Cabin Modeling. The following assumptions are used while establishing the cabin model [42]:

(1) The cabin temperature keeps constant while adjusting the pressure.

(2) The cabin volume keeps constant.

(3) The air in the cabin can be regarded as the ideal gas, and its pressure, temperature, and volume satisfy the state equation of ideal gas.

(4) The leak volume is ignored while modeling because it is much smaller than the supply and exhaust volume.

(5) The supply volume keeps constant.

Based on the assumptions (1)–(5), the differential equation of cabin pressure can be described as

$$\frac{V_c}{RT_c}\frac{\mathrm{d}P_c}{\mathrm{d}\tau} = G_K - G_B, \tag{1}$$

where V_c is the cabin volume, R is the ideal gas constant, T_c is the cabin temperature, P_c is the cabin pressure, G_k is the supply volume, and G_B is the exhaust volume.

While $P_h/P_c > 0.528$, G_B subcritical state equation is

$$G_B = \mu_B F_B \frac{0.156P_c}{\sqrt{T_c}}\sqrt{\left(\frac{P_h}{P_c}\right)^{1.43} - \left(\frac{P_h}{P_c}\right)^{1.71}}, \tag{2}$$

and while $P_h/P_c \leq 0.528$, G_B supercritical state equation is

$$G_B = \mu_B F_B \frac{0.04P_c}{\sqrt{T_c}}, \tag{3}$$

where μ_B and F_B are the flow coefficient and flow area of the exhaust valve, respectively. P_h is the atmospheric pressure.

After (1) is linearized at the equilibrium point and normalized, the cabin linearization equation can be obtained as [43, 44]

$$\left(T_{\mathrm{cp}}s + 1\right)P_c(s) = g_B F_B(s), \tag{4}$$

where T_{cp} is the cabin pressure time constant and g_B is the efficiency coefficient of influence of exhaust valve sensitivity on cabin pressure.

3.2. Drive Motor Modeling. Brushless DC motor is generally selected as the drive motor, and its equation is expressed as follows:

$$\left(T_M s^2 + s\right)\alpha_1\lambda_\alpha(s) = \frac{r}{C_e}u_0 X_u(s), \tag{5}$$

where T_M, r, C_e, and u_0 are the motor mechanical time constant, the reduction ratio of reduction machine, the motor potential constant, and the maximum armature potential, respectively. λ_α and α_1 are opening and maximum opening of the exhaust valve, respectively. X_u is the controller output voltage.

3.3. Exhaust Valve Modeling. Butterfly structure exhaust valve is adopted in this paper, and its flow area F_B calculation formula is

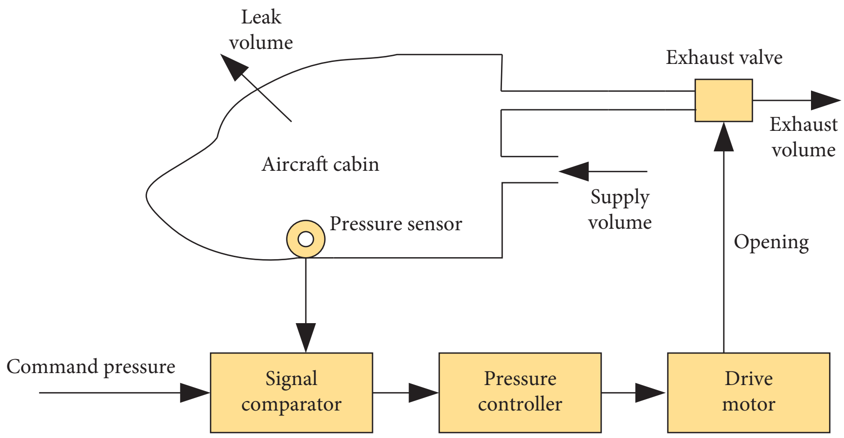

Figure 1: Structure of CPCS.

$$F_B = F_{Bg}\left(1 - \sin\lambda_\alpha\right), \tag{6}$$

where F_{Bg} is the exhaust valve maximum flow area. After equation (6) is linearized at the equilibrium point and normalized, the exhaust valve linearization equation can be obtained as [45]

$$\left(1 - \sin\alpha_0\right)F_B(s) = -\alpha_1 \cos\alpha_0 \lambda_\alpha(s), \tag{7}$$

where α_0 is the opening of the exhaust valve at the equilibrium point.

3.4. Cabin Pressure Controller Modeling. PID controller is applied because of its common and wide application in engineering:

$$X_u(t) = k_p e(t) + k_i \int e(t)\mathrm{d}t + k_d \frac{\mathrm{d}e(t)}{\mathrm{d}t}, \tag{8}$$

where e is the error of command and actual cabin pressure and k_p, k_i, k_d are the gain of proportion, integration, and differentiation, respectively.

3.5. Supplement Equation. According to the standard definition of atmosphere, the relationship between atmospheric pressure change and height is [1]

$$P_h = P_0\left(1 - \frac{h}{44330}\right)^{5.255}, \tag{9}$$

where P_0 is the atmospheric pressure at sea level.

4. Reconfiguration Design

4.1. SAC Method. In this paper, the SAC law is developed to compensate for the adverse effects caused by the fault. Control gains of the controller are adjusted online via adaptive law according to the operation process and tracking error [46–48]. The reference model can be designed as a low-order linear model. Meanwhile, there is no need to know the faulty situation in advance utilizing the SAC method to reconfigure the control system [36]. Furthermore, the SAC method also has the advantages of a simple control structure and fewer parameters to be adjusted than normal adaptive controllers. To this end, the whole closed-loop control system CPCS is regarded as the controlled object. The structure of the SAC-based reconfiguration control system is shown in Figure 2.

The mathematical model of CPCS in state-space equation form can be described as follows:

$$\begin{cases} \dot{x} = Ax + Bu, \\ y = Cx, \end{cases} \tag{10}$$

where $x \in R^n$ represents the state vector, $u \in R^s$ is the input vector, and $y \in R^q$ is the output vector. In addition, here, $A \in R^{n\times n}$, $B \in R^{n\times s}$, and $C \in R^{q\times n}$ are the system matrices.

When the faults occur in the control system, the state-space equation of CPCS can be described as follows:

$$\begin{cases} \dot{x}_p = A_p x_p + B_p u_p, \\ y_p = C_p x_p, \end{cases} \tag{11}$$

$$\begin{cases} A_p = A + \sigma A, \\ B_p = B + \sigma B, \\ C_p = C + \sigma C, \end{cases} \tag{12}$$

where $x_p \in R^{n_p}$, $u_p \in R^{s_p}$, and $y_p \in R^{q_p}$ have the same meanings as x, y, and u, respectively. In addition, here, $A_p \in R^{n_p\times n_p}$, $B_p \in R^{n_p\times s_p}$, and $C_p \in R^{q_p\times n_p}$ are the faulty system matrices. σA, σB, and σC are the bounded parameter perturbation matrices with appropriate dimensions caused by the faults.

The final control goal is to design a total control signal u_p so that all signals in the whole closed-loop system are bounded and CPCS output y_p tracks the output of the reference model given by

$$\begin{cases} \dot{x}_m = A_m x_m + B_m u_m, \\ y_m = C_m x_m, \end{cases} \tag{13}$$

where $x_m \in R^{n_m}$, $u_m \in R^{s_m}$, and $y_m \in R^{q_m}$ are the state vector, the input vector, and the output vector of the reference model, respectively. $A_m \in R^{n_m\times n_m}$, $B_m \in R^{n_m\times s_m}$, and $C_m \in R^{q_m\times n_m}$ are the system matrices of the reference model.

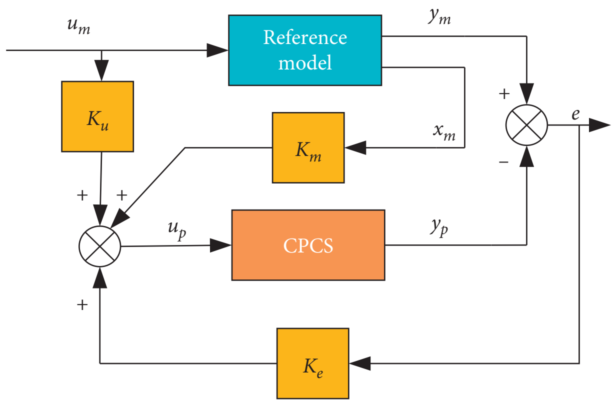

FIGURE 2: Structure of the SAC-based reconfiguration control system.

According to the structure of SAC-based reconfiguration control system, the SAC law is given by

$$u_p = K_x x_m + K_u u_m + K_e e_y, \tag{14}$$

where $K_x \in R^{s_p \times n_m}$, $K_u \in R^{s_p \times s_m}$, and $K_e \in R^{s_p \times q_m}$ are the adaptive gains and $e_y = y_m - y_p$.

The adaptive control gains can be redefined as

$$\begin{cases} K = K_P + K_I = [\, K_e \;\; K_x \;\; K_u \,] \in R^{s_p \times (n_m + s_m + q_m)}, \\ u_p = K r_m, \end{cases} \tag{15}$$

where K_P is the proportional gain and K_I is the integral gain. Both can be updated online as follows:

$$\begin{cases} K_P = e_y r_m^T T_P, \\ \dot{K}_I = e_y r_m^T T_I - \lambda K_I, \\ r_m^T = \left[e_y^T, x_m^T, u_m^T \right] \in R^{1 \times (n_m + s_m + q_m)}, \end{cases} \tag{16}$$

where

$$\begin{cases} T_P \in R^{(n_m + s_m + q_m) \times (n_m + s_m + q_m)} > 0, \\ T_I \in R^{(n_m + s_m + q_m) \times (n_m + s_m + q_m)} > 0. \end{cases} \tag{17}$$

Remark 1. The reasons for introducing proportional-integral adaptive control gain are as follows:

(i) The proportional gain has the effect of increasing the rate of convergence of the system towards perfect tracking [32, 49]. It adds an immediate penalty for large errors and leads the system very quickly towards small tracking errors.

(ii) The integral gain can enhance the stability and progressive tracking performance of the adaptive system and reduce the steady-state error.

(iii) The combination of proportional gain and integral gain can maintain the robustness of the adaptive control system in the presence of any bounded input and output disturbances.

Moreover, the λ-term is introduced in order to avoid divergence or too high value of the integral gains in the presence of disturbances.

For the system given by (11), the ideal control input can be defined as

$$u_p^* = \tilde{K}_x x_m + \tilde{K}_u u_m + \tilde{K}_e e_y, \tag{18}$$

where $\tilde{K}_x \in R^{s_p \times n_m}$ and $\tilde{K}_u \in R^{s_p \times s_m}$ are the ideal adaptive control matrices and $\tilde{K}_e \in R^{s_p \times q_m}$ is the stable tracking error gain matrix. Equation (18) can also be expressed as

$$u_p^* = \tilde{K} r_m, \tag{19}$$

where $\tilde{K} = [\, \tilde{K}_e \;\; \tilde{K}_x \;\; \tilde{K}_u \,]$.

When the ideal control u_p^* is added to the system, the output of the system can track the output of the reference model well. Then, we can obtain

$$\begin{aligned} e_y &= y_m - y_p = 0, \\ u_p^* &= \tilde{K}_x x_m + \tilde{K}_u u_m. \end{aligned} \tag{20}$$

Therefore, the ideal equation of the control system is defined as

$$\begin{aligned} & x_p^* = X_{11} x_m + X_{12} u_m, \\ & \begin{cases} \dot{x}_p^* = A_p x_p^* + B_p u_p^*, \\ y_p^* = C_p x_p^*, \end{cases} \end{aligned} \tag{21}$$

where $X_{11} \in R^{n_p \times n_m}$ and $X_{12} \in R^{n_p \times m_m}$ are the matrices satisfying the tracking matching conditions.

Then, we can obtain

$$y_p^* = C_p x_p^* = C_m x_m = y_m. \tag{22}$$

The state error equation and the differential equation of the state error can be defined as follows:

$$\begin{cases} e_x = x_p^* - x_p, \\ \dot{e}_x = \dot{x}_p^* - \dot{x}_p = \left(A_p - B_p \tilde{K}_e C_p \right) e_x - B_p (K - \tilde{K}) u_m, \\ e_y = C_p e_x. \end{cases} \tag{23}$$

Definition 1. (see [50]). The sufficient condition for the system described by $\{A_p, B_p, C_p\}$ to be strictly passive real is

$$\begin{cases} P\left(A_p - B_p \tilde{K}_e C_p \right) + \left(A_p - B_p \tilde{K}_e C_p \right) P = -Q, \\ P B_p = C_p^T, \end{cases} \tag{24}$$

where P and Q are the positive-definite symmetric matrices.

Remark 2. According to the preceding modeling and Definition 1, CPCS described by $\{A, B, C\}$ is a closed-loop control system that can be made strictly positive by the basic pressure controller. Moreover, the faulty control system described by $\{A_p, B_p, C_p\}$ can be regarded as almost strictly positive real by the next feedforward control design.

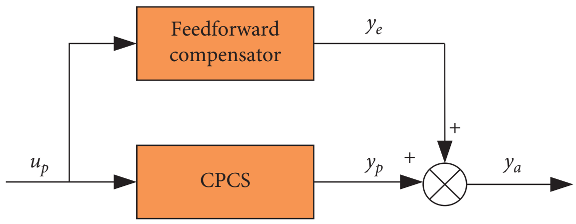

Figure 3: Structure of the controlled object.

4.2. Feedforward Control Design. When CPCS is in a normal state, the inner loop PID controller can ensure the good working quality of CPCS. When CPCS fails, the parameters of the system will be affected during operation, which will change the system's positive realness. A parallel feedforward compensator should be designed for fulfilling the condition of positive realness when the fault occurs [51]. So that the SAC-based method can be applied.

Lemma 1 (see [37]). *Assuming that $G_p(s) \in R^{m\times m}$ is any strictly real transfer function with McMillan degree, $G_p(s)$ may be not stable or minimum phase. If there exists a nonsingular constant output feedback gain K_f which makes the closed-loop transfer function*

$$G_c(s) = \left(I + G_p(s)K_f\right)^{-1}G_p(s), \tag{25}$$

asymptotically stable, then the almost strictly positive real conditions will be satisfied by the augmented open-loop transfer function which can be described as follows:

$$G_a(s) = G_p(s) + K_f^{-1}. \tag{26}$$

Lemma 2 (see [52]). *If there exist two positive symmetrical matrices P and Q and a positive real matrix $W = S^TS$, both of which satisfy the conditions*

$$P\left(A_p - B_pK_fC_p\right) + \left(A_p - B_pK_fC_p\right)^T P = -Q < 0, \tag{27}$$

$$PB_p = C_p^T W, \tag{28}$$

then the closed-loop transfer function matrix, shown as $G_p(s) = C_p(sI - A_p + B_pK_fC_p)^{-1}B_p$, is strictly positive real.

According to Definition 1, Lemmas 1 and 2, and Remark 2, we can design a parallel feedforward compensator K_f^{-1} for faulty CPCS. Thus, both the faulty closed-loop system and the augmented system with a parallel feedforward compensator are almost strictly positive. The structure of the controlled object is shown in Figure 3.

Assume that the state-space equations of CPCS with different failures can be described as follows:

$$\dot{x}_p = A_{pi}x_p + B_{pi}u_p, \; i = 1, 2, \ldots, m, \tag{29}$$

where each of the different faults corresponds to the different value of i. So that we can obtain K_{fi} which guarantees the stability of each faulty system by solving every matrix inequality in the positive real Lemma 2.

By transforming (27), we can obtain

$$\begin{aligned} A_{pi}X + XA_{pi}^T - B_{pi}Y - Y^TB_{pi}^T &< 0, \\ P = P^T &> 0, \end{aligned} \tag{30}$$

where $X = P^{-1}$ and $K_f = YPC_p^{-1}$. The feedforward gain matrix can be obtained by solving (27).

Remark 3. For this part, the feedforward gain design for every faulty system is considered a challenging condition. In other words, about actuator 80% failure and pressure sensor failure will be taken into consideration. Thus, the unified gain will keep all faulty systems stable.

4.3. Stability Analysis

Theorem 1. *All signals in the faulty CPCS can be closed-loop bounded under the controller (14) and adaptive laws (16).*

Proof. To guarantee the stability and perfect tracking performance of the adaptive control system, the following positive-definite Lyapunov function is chosen [52]:

$$V = e_x^TPe_x + \text{trace}\left[S(K_I - \tilde{K})T_I^{-1}(K_I - \tilde{K})^TS^T\right]. \tag{31}$$

Next, the time derivative of V can be obtained:

$$\begin{aligned} \dot{V} &= \dot{e}_x^TPe_x + e_x^TP\dot{e}_x \\ &\quad + \text{trace}\left\{S\left[\dot{K}_IT_I^{-1}(K_I - \tilde{K})^T + (K_I - \tilde{K})T_I^{-1}\dot{K}_I\right]S^T\right\} \\ &= e_x^T\left[P\left(A_p - B_pK_fC_p\right) + \left(A_p - B_pK_fC_p\right)^TP\right]e_x \\ &\quad + e_x^TPB_p\tilde{K}r_m - e_x^TPB_pKr_m + e_y^TS^TS(K_I - \tilde{K})r_m \\ &= e_x^T\left[P\left(A_p - B_pK_fC_p\right) + \left(A_p - B_pK_fC_p\right)^TP\right]e_x \\ &\quad + e_x^TPB_p\tilde{K}r_m - e_x^TPB_pKr_m + e_x^TC_p^TS^TS(K_I - \tilde{K})r_m. \end{aligned} \tag{32}$$

Then, we substitute (16) and (28) into (32):

$$\begin{aligned} \dot{V} &= e_x^T\left[P\left(A_p - B_pK_fC_p\right) + \left(A_p - B_pK_fC_p\right)^TP\right]e_x - e_x^TPB_pK_pr_m \\ &= e_x^T\left[P\left(A_p - B_pK_fC_p\right) + \left(A_p - B_pK_fC_p\right)^TP\right]e_x - e_x^TPB_pC_pe_xr_m^TT_Pr_m \\ &= e_x^T\left[P\left(A_p - B_pK_fC_p\right) + \left(A_p - B_pK_fC_p\right)^TP\right]e_x - e_x^TPB_p\left(S^TS\right)^{-1}B_p^TPe_xr_m^TT_Pr_m. \end{aligned} \tag{33}$$

According to (27), which is fulfilled by designing the feedforward compensator,

$$\dot{V} < 0. \tag{34}$$

Through the above analysis, the stability of SAC-based configuration system has been guaranteed. □

5. Simulation Results

In this section, we show the results obtained in a series of simulations to verify the effectiveness and reconfiguration control capability of the proposed method. The reconfiguration control system for CPCS is built based on MATLAB/Simulink software, and the values of model parameters are shown in Table 1.

According to the previous modeling, the CPCS can be rewritten as the state-space model:

$$\begin{cases} \dot{x} = Ax + Bu, \\ y = Cx, \end{cases} \tag{35}$$

where $x = [f_B, \ddot{X}_u, \dot{X}_u, X_u]^T \in R^4$ is the state vector and f_B is the integral value of F_B. $y = [P_c] \in R^1$ is the output vector of the system. The input vector $u = [P_{cd}] \in R^1$, and P_{cd} is the command cabin pressure value. In addition, the following system matrices can be obtained:

$$\begin{aligned} A &= \begin{bmatrix} -0.0037 & -6.3268 \times 10^4 & -5.6391 \times 10^4 & -1.2379 \times 10^4 \\ 0.0019 & -147.0588 & 0 & 0 \\ 0 & 1 & 0 & 0 \\ 0 & 0 & 1 & 0 \end{bmatrix}, \\ B &= \begin{bmatrix} 0 & 1 & 0 & 0 \end{bmatrix}^T, \\ C &= \begin{bmatrix} -0.0019 & 0 & 0 & 0 \end{bmatrix}. \end{aligned} \tag{36}$$

The system matrices $\{A_m, B_m, C_m\}$ of the reference model chosen in this paper are equal to the above $\{A, B, C\}$. The faulty CPCS model is the same as (11).

Remark 4. The identity matrix is generally selected as the value of the proportional gain and the integral gain [36, 47, 48]. In this paper, the reconfiguration effects of the faulty CPCS are taken into consideration, which include the reconfiguration speed and the oscillation situation. Therefore, the proportional-integral gain value should be adjusted accordingly compared with other pieces of literature.

As a result, the parameters of the simple adaptive controller in (16) are chosen as follows:

$$\begin{aligned} T_P &= \begin{bmatrix} 0.001 & 0 & 0 & 0 & 0 & 0 \\ 0 & 0 & 0 & 0 & 0 & 0 \\ 0 & 0 & 25 & 0 & 0 & 0 \\ 0 & 0 & 0 & 20 & 0 & 0 \\ 0 & 0 & 0 & 0 & 26 & 0 \\ 0 & 0 & 0 & 0 & 0 & 0.001 \end{bmatrix}, \\ T_I &= \begin{bmatrix} 0.01 & 0 & 0 & 0 & 0 & 0 \\ 0 & 0 & 0 & 0 & 0 & 0 \\ 0 & 0 & 58 & 0 & 0 & 0 \\ 0 & 0 & 0 & 50 & 0 & 0 \\ 0 & 0 & 0 & 0 & 10 & 0 \\ 0 & 0 & 0 & 0 & 0 & 0.0005 \end{bmatrix}, \\ \lambda &= 0.0001. \end{aligned} \tag{37}$$

The feedforward control gain $K_f = 3310.3158$ which is obtained by using the MATLAB LMI toolbox.

To be close to the real situation, the entire flight envelope of the aircraft from take-off to landing is designed in this paper. The flight height is shown in Figure 4, and the flight height function is as follows:

$$h = \begin{cases} 0, & 0 \le t < 250, \\ 10(t - 250), & 250 \le t < 1450, \\ 12000, & 1450 \le t < 1950, \\ -10(t - 1950) + 12000, & 1950 \le t < 3150, \\ 0, & 3150 \le t < 3500, \end{cases} \tag{38}$$

where h is the flight height and t is the flight time.

The pressure schedule applied in this paper is

$$P_{cd} = P_h + \frac{1}{1.5583}(P_0 - P_h) + 3300, \tag{39}$$

where P_{cd} is the command cabin pressure value, P_h is the atmospheric pressure, and P_0 is the atmospheric pressure at sea level.

5.1. CPCS with No-Fault.

The pressure response test of CPCS with no-fault throughout the entire flight envelope is shown in Figure 5. The results highlight that CPCS with no-fault has excellent performance of pressure tracking, which can ensure the safety of flight crew. Moreover, the reference model selected in this paper satisfies the requirement of the usual selection.

5.2. CPCS with Pressure Senor Fault.

Among aircraft cabin pressure accidents, the number of accidents during the cruise phase was 174, which accounted for 46.8% [4]. For

Table 1: Values of model parameters.

Symbols	Descriptions	Values
T_{cp}	Cabin pressure time constant	268.17 s
g_B	Efficiency coefficient of influence of exhaust valve sensitivity on cabin pressure	−0.511
T_M	Motor mechanical time constant	0.0068 s
r	Reduction ratio of reduction machine	0.001
C_e	Motor potential constant	0.025 V · s/rad
u_0	Maximum armature potential	24 V
α_1	Maximum opening of the exhaust valve	$\pi/2$
α_0	Opening of the exhaust valve at the equilibrium point	$\pi/5$
k_p	Gain of proportion	205
k_i	Gain of integration	45
k_d	Gain of differentiation	230
P_0	Atmospheric pressure at sea level	101,325 Pa

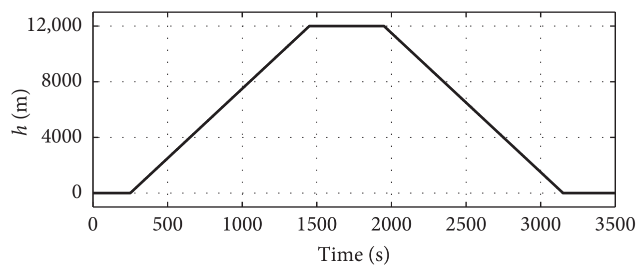

Figure 4: Relationship between flight height and time.

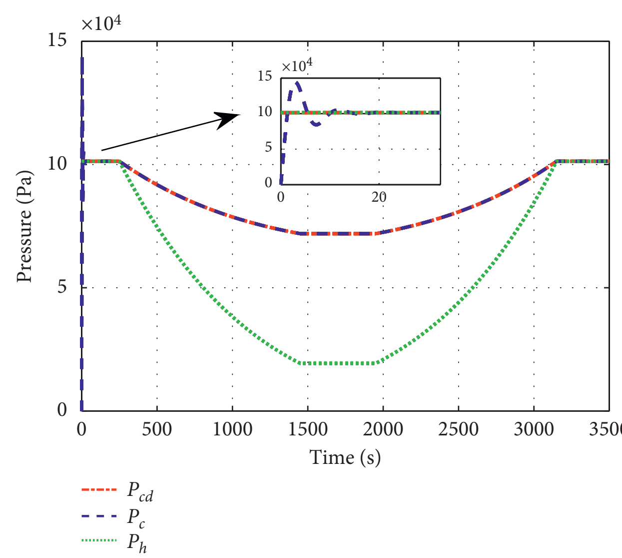

Figure 5: Pressure response of CPCS in the entire flight envelope.

this reason, the reconfiguration test for CPCS with pressure sensor faults is carried out during the cruise phase.

The pressure sensor has constant gain drift at 1500 s when the aircraft is cruising at 12000 m, while the pressure error P_e between the reference model and the cabin without reconfiguration is shown in Figure 6, where d is the constant gain coefficient. As detailed in Figure 6, P_e caused by the constant gain drift of the sensor is so huge that the safety of the crew will be threatened. Furthermore, we consider the situation of the pressure sensor failure (same as $d = 0$), and the result of this test is presented in Figure 7. The aircraft structure might be directly destroyed by the huge pressure error.

Then, the proposed method is tested in each of these cases. P_e and u_p after reconfiguration are shown in Figure 8. From Figure 8, it can be noted that the proposed method has an excellent reconfiguration performance which can ensure the safety of the crew and the aircraft. The results shown here confirm the rapid self-repairing control ability of the proposed method under pressure sensor faults.

5.3. CPCS with Actuator Fault. Given the study design chosen, it is inevitable that CPCS has no functional redundancy because of SISO characteristics. If the CPCS actuator fails completely, it can only be reconfigured at the hardware structure level, such as redundancy design [53]. Thus, we only test the proposed method in the case of the CPCS actuator partial failure. More often than not, the time spent in the take-off and climbing phases accounts for 15%

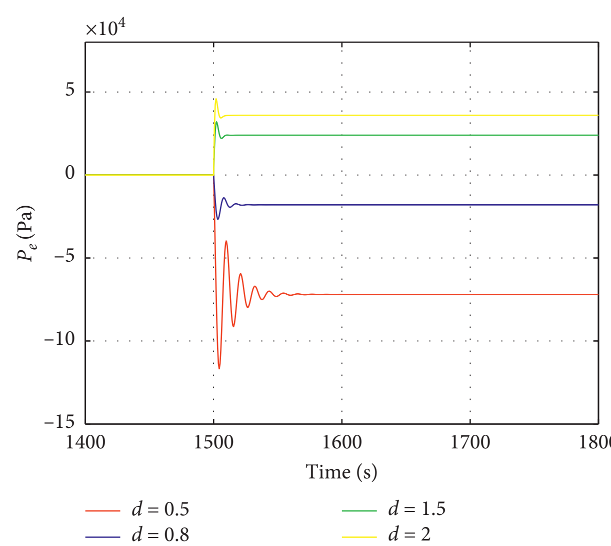

Figure 6: Pressure error caused by the constant gain drift of the pressure sensor.

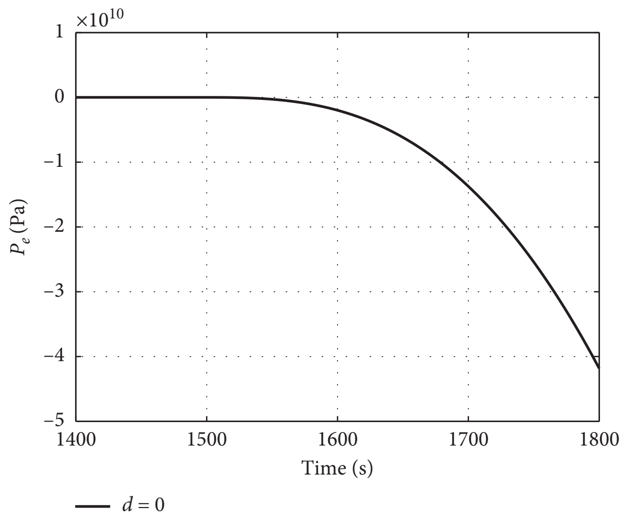

Figure 7: Pressure error caused by the pressure sensor failure.

of the entire flight segment, and the accident rate was 27.7% [4]. To this end, the reconfiguration test for CPCS with actuator partial failure is carried out during the climbing phase.

The actuator partial failure occurs at 350 s when the aircraft is climbing to 1000 m. And P_e without reconfiguration is reported in Figure 9. As can be seen in Figure 9, P_e will be convergence after a slight oscillation in the cases of the actuator 20% and 50% failure. This is caused by the basic pressure controller. However, at 80% failure, the effect of the pressure controller seems weak and P_e oscillates violently and diverges that will cause serious consequences.

To verify the proposed method under the above cases, some simulations are carried out. P_e and u_p after reconfiguration are presented in Figure 10. Not only is the reconfiguration speed fast, but also the reconfiguration performance is excellent. To conclude, the results of this section stress that the SAC-based reconfiguration system can effectively eliminate the adverse effects caused by the faults mentioned above.

5.4. CPCS with Double Faults. Since the above simulations only test the proposed method for a single fault, we will verify its effectiveness under double faults. The proposed method is tested during the descent phase in this section.

Firstly, 0.8 gain drift occurs in the pressure sensor at 2500 s when the aircraft is descending to 6500 m. Then 50% of the failure occurs in the actuator at 2600 s. Secondly, the above two faults occur simultaneously at 2500 s. P_e of these cases without reconfiguration are shown in Figures 11 and 12, respectively. As we can see, the impact of double faults is more violent compared to that of single fault. This will not only cause great trouble to the pilot's work but also affect flight safety and endanger the crew's lives and property.

To test the effectiveness of the proposed method under the above situations, simulations are carried out. As detailed in Figures 13 and 14, in the case of simultaneous and sequential occurrence of double faults, the output of CPCS can effectively achieve the tracking of the reference model. Although there are some slight oscillations of the cabin pressure after reconfiguration, this condition is normal. The aircraft is in a descending state, and the atmospheric pressure continues to rise. Similarly, the command cabin pressure value is constantly changing so that there will be a small and changing gap between the reference model and the faulty CPCS after reconfiguration. This is the cause of the slight oscillations. In summary, these results emphasize the validity of the proposed method, which can achieve a satisfying performance in the case of double faults.

5.5. Simulation Comparison. A simulation comparison is conducted in this section. A traditional Model Following (MF) method [54] and a Model Following Direct Adaptive Control method (MFDAC) proposed by Chai et al. [28] are imported into the comparison.

Firstly, the constant gain drift ($d = 0.8$) occurs in the pressure sensor at 1500 s. Figure 15 shows a considerable difference between the three methods. As we can see, MF causes a chattering at the fault point and a steady-state error whose value is around 100 Pa. Although P_e after MFDAC reconfiguration does not make the chattering, the slightly larger pressure error oscillation and the slow convergence are not satisfying. Compared with the above methods, SAC has a better reconfiguration performance, including fast convergence, no chattering, and no oscillation. Therefore, the method proposed in this paper is more effective for CPCS sensor faults compared with MF and MFDAC.

Secondly, the partial failure (50%) occurs in the actuator at 350 s. The result of this test is presented in Figure 16. As shown in Figure 16, except the unsatisfying chattering caused by MF, no noteworthy differences are found between the three methods. The reconfiguration performances are excellent enough. These three methods are all effective for CPCS actuator faults. Also, a limitation of MF is found: MF needs to adjust reconfiguration parameters according to the fault situation to meet the demand. This may limit its application in actual systems.

The results of this section highlight the effectiveness and advantages of SAC. In conclusion, the proposed method in this paper can more effectively handle the various potential faults in CPCS compared with the above methods.

5.6. External Disturbance Simulation. In this section, the proposed method is investigated with different higher amplitudes of external disturbances. The output disturbance d_o can be described as follows [32]:

$$d_o = A \sin(\omega t + \varphi), \tag{40}$$

where A is the amplitude, ω is the frequency, and φ is the phase.

When the failure of the pressure sensor occurs ($t = 1500$ s), d_o is added to the output of CPCS. Three different higher amplitudes of output disturbances are selected in this paper: (1) $\begin{cases} A = 50 \\ \omega = 4 \\ \varphi = 0 \end{cases}$; (2) $\begin{cases} A = 100 \\ \omega = 4 \\ \varphi = 0 \end{cases}$;

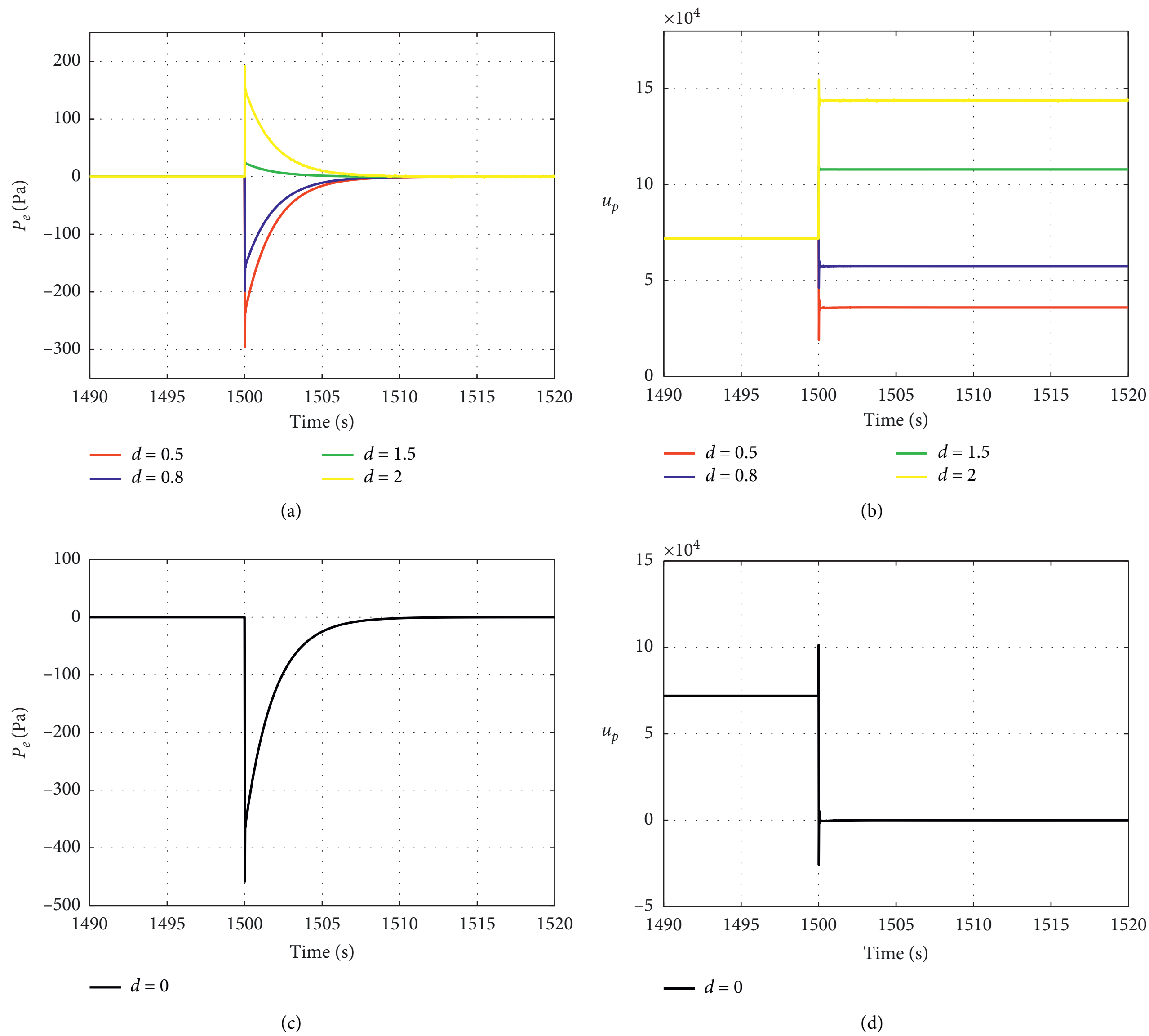

Figure 8: Pressure error and control input of pressure sensor faults after reconfiguration.

(3) $\begin{cases} A = 200 \\ \omega = 4 \\ \varphi = 0 \end{cases}$, which are shown in Figure 17. P_e and u_p of the three situations after reconfiguration are shown in Figure 18.

From Figure 18, it can be noted that the proposed method has a good reconfiguration performance under the output disturbances. As the amplitude of the output disturbance increases, P_e produces a slight chattering that can be ignored. Besides, the reconfiguration speed is less affected by disturbances. In conclusion, an excellent antidisturbance ability of the proposed method is indicated by simulation results.

5.7. Summary. In summary, several typical faults are selected for the reconfiguration research of CPCS. After analyzing the above simulation results, the importance of CPCS health can be realized. The proposed method can rapidly reconfigure the faulty system without knowing the faulty situation ahead of time, and its reconfiguration performance is satisfying.

Remark 5. T_P and T_I are mainly used to adjust the adaptive law. After various simulation studies, the control parameters of the proposed method can be selected according to the following principles:

(i) Both reconfiguration speed and pressure error at the reconfiguration point need to be considered in the debugging process of the above two parameters. T_P can improve the convergence speed of the reconfiguration system. And T_I can not only enhance the stability and progressive tracking performance of the adaptive system but also reduce the steady-state tracking error after reconfiguration.

(ii) The oscillation after reconfiguration also should be an evaluation index for control parameter selection.

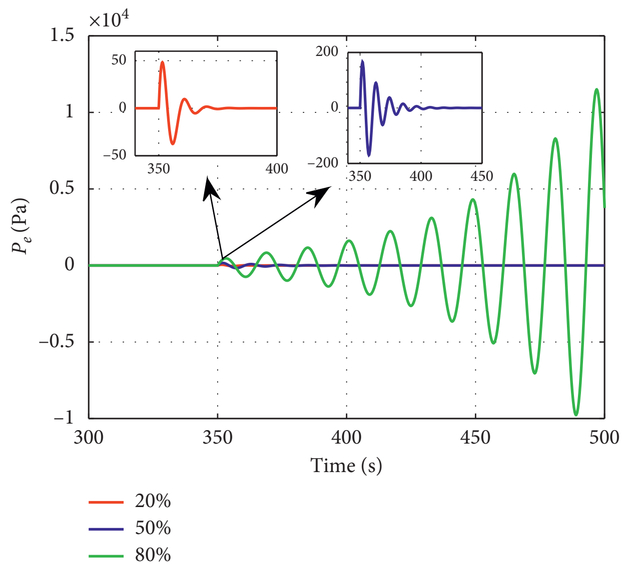

FIGURE 9: Pressure error caused by the actuator partial failure.

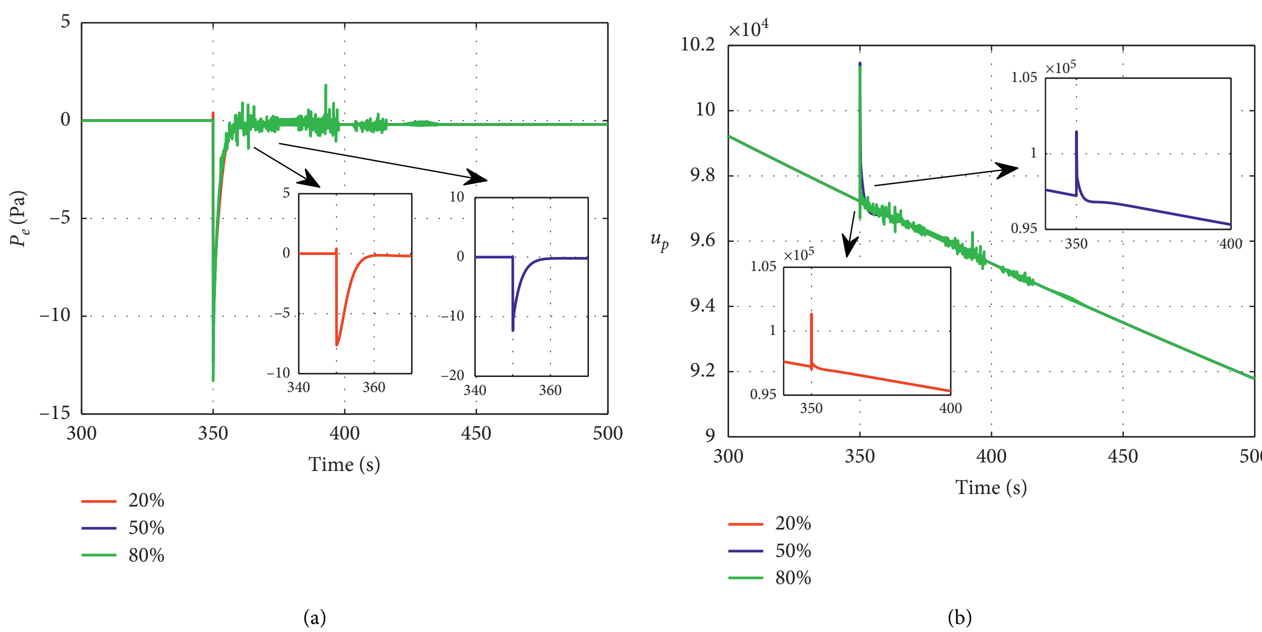

FIGURE 10: Pressure error and control input of actuator partial failure after reconfiguration.

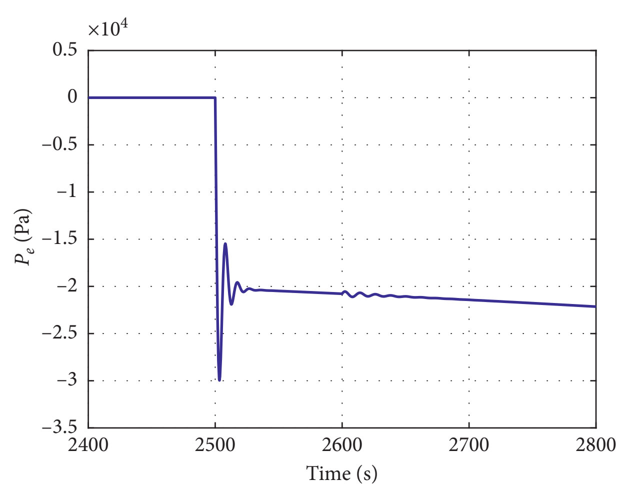

FIGURE 11: Pressure error caused by the sequential double faults.

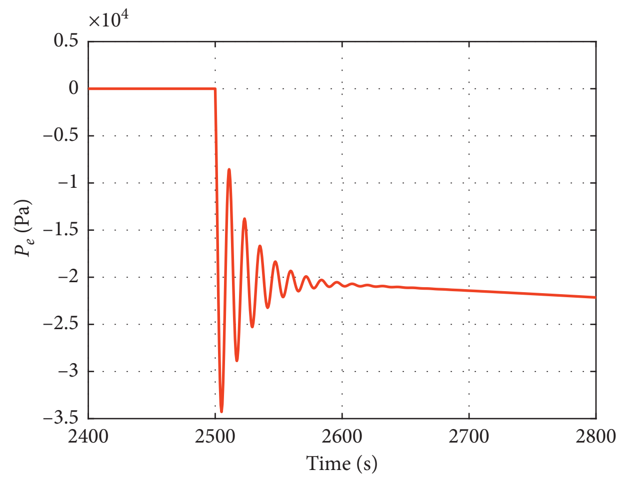

FIGURE 12: Pressure error caused by the simultaneous double faults.

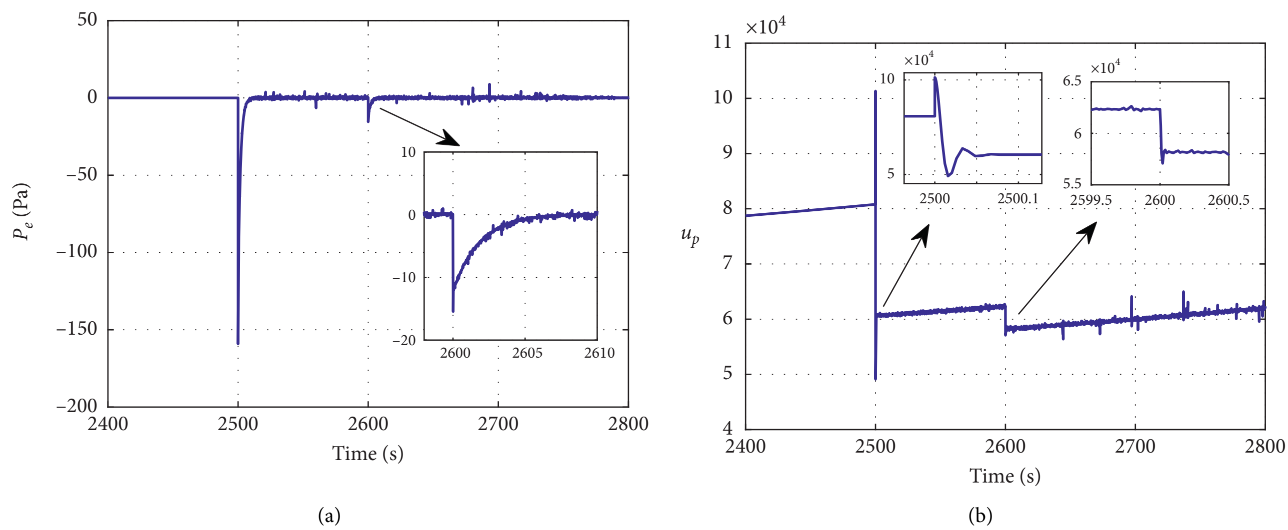

FIGURE 13: Pressure error and control input of sequential double faults after reconfiguration.

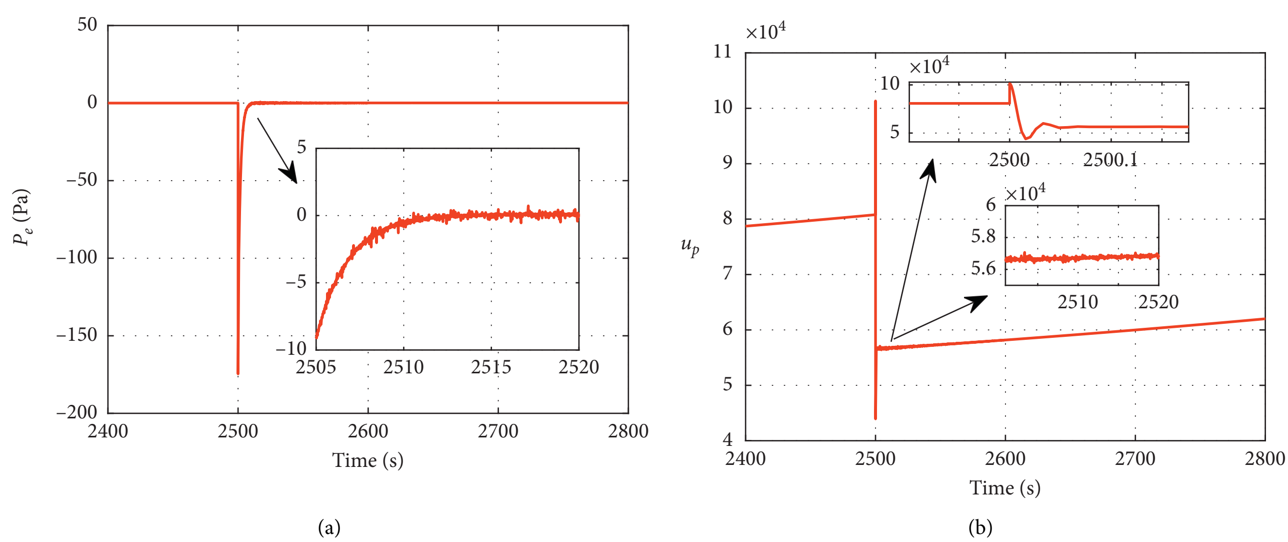

FIGURE 14: Pressure error and control input of simultaneous double faults after reconfiguration.

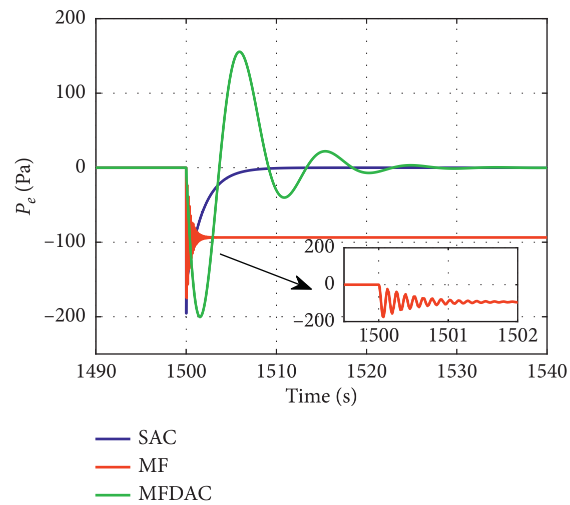

Figure 15: Pressure error of the sensor fault after reconfiguration.

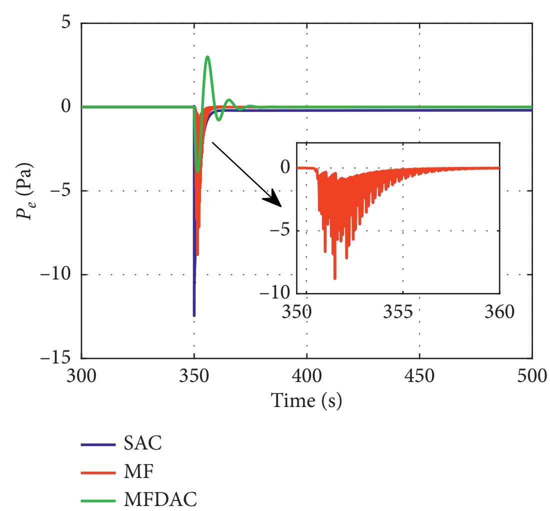

Figure 16: Pressure error of the actuator fault after reconfiguration.

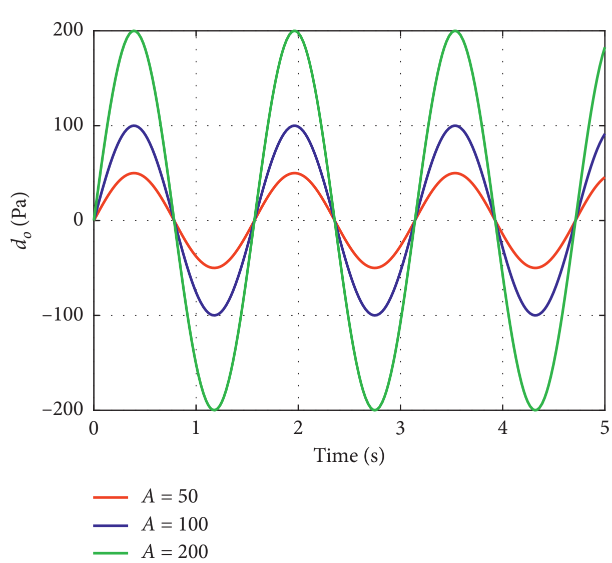

Figure 17: Different higher amplitudes of output disturbances d_o.

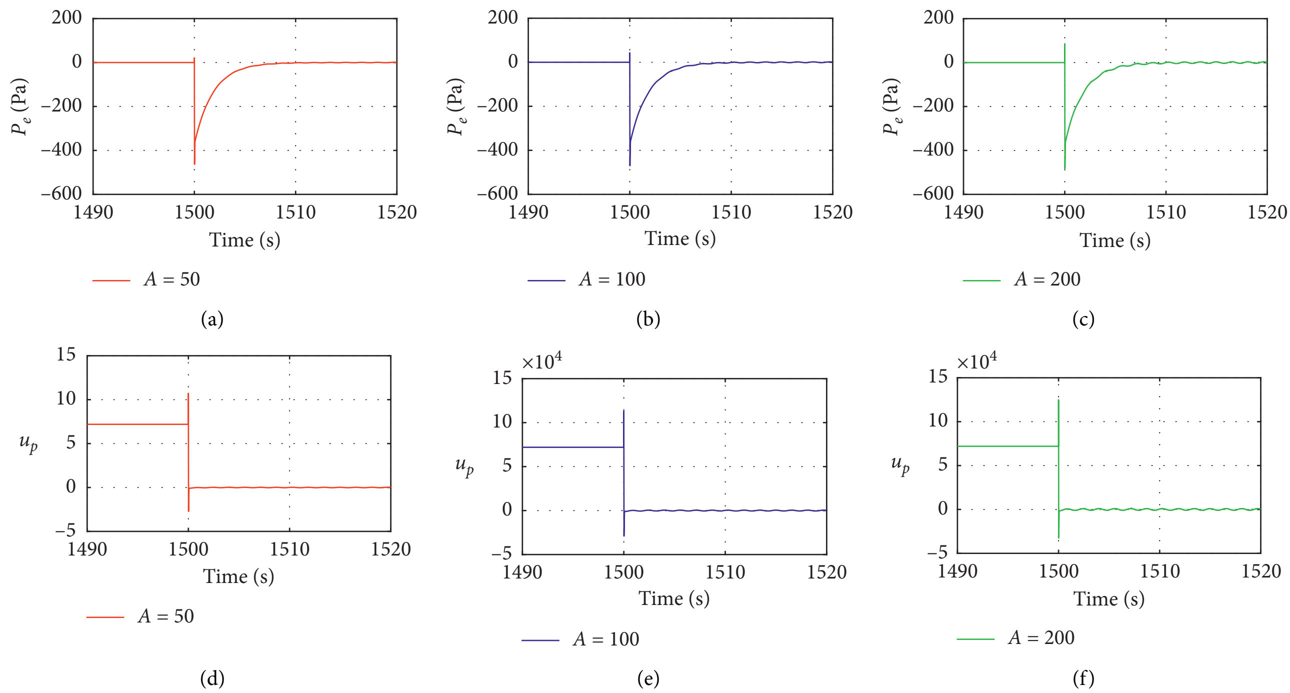

Figure 18: Pressure error and control input of three situations after reconfiguration.

Violent oscillation is undesirable in the reconfiguration process. A proper combination of T_P and T_I can reduce and even eliminate the oscillation and maintain the robustness of the reconfiguration system when the fault occurs in CPCS.

6. Conclusion

Normal operation of CPCS is a basic condition for the successful completion of a flight mission. A SAC-based reconfiguration design of CPCS has been proposed in this paper. The CPCS mathematical model is given by considering the mechanical characteristics of CPCS. The pressure controller of CPCS ensures the performance of pressure control in normal operation. The utilization of SAC is to get good pressure tracking capability of CPCS under faults. And a parallel feedforward compensator is designed to meet the almost strictly positive real conditions. The simulation results of this study suggest that the proposed method has a good reconfiguration capability for CPCS under different faults. And the robustness and the disturbance rejection have been verified.

Future work will focus on the following points:

(i) Analyze the implementation complexity of the developed controller. First of all, the proposed method greatly reduces the complexity and difficulty of implementation compared with other adaptive controls. Secondly, there are many FPGA-based reconfiguration projects for [55, 56]. Thus, the proposed method can be designed based on them.

(ii) Combine SAC with advanced control methods. As we know, sliding mode control is a robust control method that is very effective against the model uncertainties and external disturbances. In recent years, some advanced methods of sliding mode control have been proposed, such as a new integral sliding mode control [57] and a fuzzy integral sliding mode control [58]. SAC can be combined with the sliding mode technique to study the related reconfiguration problem in future research activities.

(iii) Introduce the proposed method to other AECS. According to the analysis in the introduction, AECS, including CPCS, have a lot in common. Future studies are recommended to carry out reconfiguration research on other AECS.

Data Availability

All the data used to support the findings of this study are included within the article.

Conflicts of Interest

The authors declare that this paper has no conflicts of interest.

Acknowledgments

This study was supported by the Key Laboratory Projects of Aeronautical Science Foundation of China (201928052006 and 20162852031) and the Research Innovation Program for

Postgraduates of Universities in Jiangsu Province (KYLX16_0380).

References

[1] Y. WU and D. L. Zhang, "Modeling and performance analysis of digital electronic-pneumatic cabin pressure control system," *Journal of Nanjing University of Aeronautics and Astronautics*, vol. 40, no. 3, pp. 324–328, 2008.

[2] L. Zhu, Y. Fu, J. Zhao, and D. Guo, "Research on the controller of the digital cabin pressure regulating system based on the fuzzy gain scheduling," in *Proceedings of the 2009 9th International Conference on Electronic Measurement & Instruments*, pp. 3494–3498, Beijing, China, August 2009.

[3] Z. Wei-Yi, Z. Tai-Feng, and Y. Xiao-Hua, "Analysis of typical failures of aircraft environmental control system," *Equipment Environmental Engineering*, vol. 9, no. 2, pp. 82–84, 2012.

[4] W.-y. Dai, "Aircraft cabin pressure control system failure analysis," *Equipment Manufacturing Technology*, vol. 3, pp. 75–78, 2018.

[5] T. Jiang and H. R. Zhang, "Prevention maintenance and control of analog cabin pressure control system components for B737CL," *Aviation Maintenance & Engineering*, vol. 6, no. 31, pp. 78–80, 2013.

[6] L. Ping, Z. Lei, Z. Jing-Quan et al., "Failure analysis of aircraft cabin pressure control system," in *Proceedings of the 2011 International Conference on Electronics, Communications and Control (ICECC)*, pp. 1456–1459, Ningbo, China, September 2011.

[7] N. Jinfang, P. Quan, S. Hao et al., "Design and experimental evaluation of PID controller for digital electro-pneumatic cabin pressure control system," *Transactions of Nanjing University of Aeronautics and Astronautics*, vol. 33, no. 5, pp. 576–584, 2016.

[8] L. F. Fu, G. L. Tian, B. Liang et al., "Real time modeling and simulation of aircraft cabin pressure control system," *Computer Simulation*, vol. 33, no. 02, pp. 61–64, 2016.

[9] L. Zhu, Y. L. Fu, J. Q. Zhao et al., "Fuzzy sliding mode variable structure control of digital cabin pressure regulating system," *Journal of Applied Sciences*, vol. 27, no. 5, pp. 545–550, 2009.

[10] B. Karimi, E. Zeinaly, G. Shahgholian, and S. M. A. Bahreini, "Nonaffine-Nonlinear adaptive control of an aircraft cabin pressure system using neural networks," *Journal of Aerospace Engineering*, vol. 27, no. 3, pp. 597–603, 2014.

[11] Y. Zhang and J. Jiang, "Bibliographical review on reconfigurable fault-tolerant control systems," *Annual Reviews in Control*, vol. 32, no. 2, pp. 229–252, 2008.

[12] S. Yin, B. Xiao, S. X. Ding, and D. Zhou, "A review on recent development of spacecraft attitude fault tolerant control system," *IEEE Transactions on Industrial Electronics*, vol. 63, no. 5, pp. 3311–3320, 2016.

[13] Y. Zhang, Z. Li, Z. Cheng, L. Liu, and Y. Wang, "Attitude tracking control reconfiguration for space launch vehicle with thrust loss fault," *IEEE Access*, vol. 7, pp. 184353–184364, 2019.

[14] S. X. Li, Z. Fang, and P. Li, "Control reconfiguration design for control surface fault of small unmanned aerial vehicle," *Computer Engineering and Applications*, vol. 47, no. 7, pp. 236–240, 2011.

[15] A. Boche, J.-L. Farges, and H. De Plinval, "Reconfiguration control method for non-redundant actuator faults on unmanned aerial vehicle," *Proceedings of the Institution of Mechanical Engineers, Part G: Journal of Aerospace Engineering*, vol. 234, no. 10, pp. 1597–1610, 2020.

[16] Q. Shen, C. Yue, C. H. Goh, and D. Wang, "Active fault-tolerant control system design for spacecraft attitude maneuvers with actuator saturation and faults," *IEEE Transactions on Industrial Electronics*, vol. 66, no. 5, pp. 3763–3772, 2019.

[17] Z. Gao, B. Jiang, P. Shi, J. Liu, and Y. Xu, "Active fault-tolerant tracking control for near-space vehicle attitude dynamics with actuator faults," *Proceedings of the Institution of Mechanical Engineers, Part I: Journal of Systems and Control Engineering*, vol. 225, no. 3, pp. 413–422, 2011.

[18] Q. Yang, S. S. Ge, and Y. Sun, "Adaptive actuator fault tolerant control for uncertain nonlinear systems with multiple actuators," *Automatica*, vol. 60, pp. 92–99, 2015.

[19] G. Tao, *Adaptive Control Design and Analysis*, John Wiley and Sons, Hoboken, NJ, USA, 2003.

[20] Y. Pan, P. Du, H. Xue, and H. Lam, "Singularity-free fixed-time fuzzy control for robotic systems with user-defined performance," *IEEE Transactions on Fuzzy Systems*, 2020.

[21] H. Liang, X. Guo, Y. Pan, and T. Huang, "Event-triggered fuzzy bipartite tracking control for network systems based on distributed reduced-order observers (revised manuscript of TFS-2019-1049)," *IEEE Transactions on Fuzzy Systems*, 2020.

[22] H. Liang, G. Liu, H. Zhang, and T. Huang, "Neural-network-based event-triggered adaptive control of nonaffine nonlinear multiagent systems with dynamic uncertainties," *IEEE Transactions on Neural Networks and Learning Systems*, 2020.

[23] H. Kaufman, "Direct adaptive control algorithms," *Direct Adaptive Control Algorithms: Theory and Applications*, Springer-Verlag New York, Inc., New York, NY, USA, 1994.

[24] B. Jiang, Y. Guo, and P. Shi, "Adaptive reconfiguration scheme for flight control systems," *Proceedings of the Institution of Mechanical Engineers, Part I: Journal of Systems and Control Engineering*, vol. 224, no. 6, pp. 713–723, 2010.

[25] M. Bodson and J. E. Groszkiewicz, "Multivariable adaptive algorithms for reconfigurable flight control," *IEEE Transactions on Control Systems Technology*, vol. 5, no. 2, pp. 217–229, 1997.

[26] M. Bodson and W. A. Pohlchuck, "Command limiting in reconfigurable flight control," *Journal of Guidance, Control, and Dynamics*, vol. 21, no. 4, pp. 639–646, 1998.

[27] K. S. Kim, K. J. Lee, and Y. Kim, "Reconfigurable flight control system design using direct adaptive method," *Journal of Guidance Control & Dynamics*, vol. 26, no. 4, pp. 543–550, 2012.

[28] S. L. Chai, S. Q. Liu, Y. J. Fan et al., "Model-following direct adaptive control based reconfigurable control design for failures of a jumbo jet transport aircraft," *Information and Control*, vol. 42, no. 5, pp. 639–644, 2013.

[29] K. Sobel, H. Kaufman, and L. Mabius, "Implicit adaptive control for a class of MIMO systems," *IEEE Transactions on Aerospace and Electronic Systems*, vol. AES-18, no. 5, pp. 576–590, 1982.

[30] K. Sobel and H. Kaufman, "Direct model reference adaptive control for a class of MIMO systems," *Control and Dynamic Systems*, vol. 24, no. 3, pp. 245–314, 1986.

[31] I. Bar-Kana, "Direct multivariable adaptive control with application to large structural systems (microform)," Ph.D. thesis, 1983.

[32] I. Bar-Kana and H. Kaufman, "Simple adaptive control of large flexible space structures," *IEEE Transactions on Aerospace and Electronic Systems*, vol. 29, no. 4, pp. 1137–1149, 1993.

[33] S. H. Cho and R. Burton, "Position control of high performance hydrostatic actuation system using a simple adaptive

control (SAC) method," *Mechatronics*, vol. 21, no. 1, pp. 109–115, 2011.

[34] Y. I. Son, G.-J. Jeong, and I. H. Kim, "A combined simple adaptive control with disturbance observer for a class of time-delay systems," *IEICE Transactions on Fundamentals of Electronics, Communications and Computer Sciences*, vol. E93-A, no. 2, pp. 553–556, 2010.

[35] M. I. Mufti, "Model reference adaptive control for large structural systems," *Journal of Guidance Control & Dynamics*, vol. 10, no. 5, pp. 507–509, 2012.

[36] F. Chen, Q. Wu, B. Jiang, and G. Tao, "A reconfiguration scheme for quadrotor helicopter via simple adaptive control and quantum logic," *IEEE Transactions on Industrial Electronics*, vol. 62, no. 7, pp. 4328–4335, 2015.

[37] A. I. Belkharraz and K. Sobel, "Direct adaptive control for aircraft control surface failures during gust conditions," in *Proceedings of the AIAA Guidance, Navigation, and Control Conference and Exhibit*, pp. 534–547, Providence, RI, USA, August 2004.

[38] M. Takahashi, "Simple adaptive control against sensor failures," *IFAC-PapersOnLine*, vol. 52, no. 29, pp. 55–60, 2019.

[39] Z. Jian, H. Guihe, and Z. Jing, "Cabin temperature control system simulation of transportation aircraft," in *Proceedings of the 2013 Third International Conference on Instrumentation, Measurement, Computer, Communication and Control*, pp. 1689–1692, Shenyang, China, September 2013.

[40] J. Na, Y. Li, Y. Huang, G. Gao, and Q. Chen, "Output feedback control of uncertain hydraulic servo systems," *IEEE Transactions on Industrial Electronics*, vol. 67, no. 1, pp. 490–500, 2020.

[41] M. S. Pavan, J. J. Vyas, and G. Balamurugan, "Modelling and simulation of aircraft nose wheel steering system," in *Proceedings of the 2015 39th National Systems Conference (NSC)*, pp. 1–5, Noida, India, December 2015.

[42] J. Wang and X. Yang-he, *Air Parameters Control of Aircraft Cabin*, pp. 212–230, National Defense Industry Press, Beijing, China, 1980.

[43] L. Zhu, Y. Fu, and J. Zhao, "Research on the controller of the digital cabin pressure regulating system based on FIMF," in *Proceedings of the 2010 2nd International Conference on Advanced Computer Control*, pp. 454–458, Shenyang, China, March 2010.

[44] C. Liu and H. X. Wu, "Application of fuzzy control in digital cabin pressure control system," *Popular Science & Technology*, vol. 114, no. 2, pp. 108–110, 2009.

[45] K. Cheng and H. X. Wu, "Simulation of digital cabin pressure control system," *Popular Science & Technology*, vol. 125, no. 1, pp. 128–130, 2010.

[46] Q. I. Xiao-hui, Z.-j. Yang, and W. U. Xiao-bei, "The reconfigurable flight control design of adaptive sliding mode control based on simple adaptive control," *Flight Dynamics*, vol. 28, no. 4, pp. 37–41, 2010.

[47] Z.-j. Yang, Q. I. Xiao-hui, and S. Gan-lin, "A simple adaptive reconfigurable control method for aircraft control surface loss-of-effectiveness failures," *Information and Control*, vol. 38, no. 3, pp. 349–364, 2009.

[48] Q. I. Xiao-hui, Z.-j. Yang, and W. U. Xiao-bei, "Study on robust reconfigurable flight control law based on simple adaptive control," *Acta Armamentarii*, vol. 30, no. 12, pp. 1733–1737, 2009.

[49] I. Bar-Kana, "Adaptive control: a simplified approach," *Control and Dynamic Systems*, vol. 25, pp. 187–235, 1987.

[50] I. Barkana, Comments on "Design of strictly positive real systems using constant output feedback"," *IEEE Transactions on Automatic Control*, vol. 49, no. 11, pp. 2091–2093, 2004.

[51] A. Cano and K. Sobel, "Simple adaptive delta operator aircraft flight control for accommodation of loss of control effectiveness," *Engineering*, vol. 8, no. 4, pp. 173–195, 2016.

[52] I. Barkana, "Gain conditions and convergence of simple adaptive control," *International Journal of Adaptive Control and Signal Processing*, vol. 19, no. 1, pp. 13–40, 2005.

[53] Y. P. Yao and P. Q. Li, *Reliability and Redundancy Technology*, Aviation Industry Press, Beijing, China, 1991.

[54] X. H. Qi and Z. J. Yang, "Design of reconfigurable flight control based on linear model following," *Journal of Ordnance Engineering College*, vol. 20, no. 1, pp. 24–26, 2008.

[55] M. Kirchhoff, P. Kerling, D. Streitferdt, and W. Fengler, "A real-time capable dynamic partial reconfiguration system for an application-specific soft-core processor," *International Journal of Reconfigurable Computing*, vol. 2019, Article ID 4723838, 14 pages, 2019.

[56] N. Uchevlerbahram and K. Svarstad, "Modelling and assertion-based verification of run-time reconfigurable designs using functional programming abstractions," *International Journal of Reconfigurable Computing*, vol. 2018, Article ID 3276159, 25 pages, 2018.

[57] Y. Wang, Y. Xia, H. Li, and P. Zhou, "A new integral sliding mode design method for nonlinear stochastic systems," *Automatica*, vol. 90, pp. 304–309, 2018.

[58] Y. Wang, X. Xie, M. Chadli, S. Xie, and Y. Peng, "Sliding mode control of fuzzy singularly perturbed descriptor systems," *IEEE Transactions on Fuzzy Systems*, 2020.